URSI GASS 2021, Rome, Italy, 28 August - 4 September 2021

A Proposed Vacuum Window for DVA-2 Q-band receiver and ngVLA Band-5

S. Salem Hesari *(1), D. Henke (1), and L. B. G. Knee (1)
(1) NRC Herzberg Astronomy and Astrophysics Research Centre
Victoria, BC, V9E 2E7, Canada

Abstract

The Q-band receiver development for DVA-2 and ngVLA band-5 optics require a high efficiency vacuum window that covers the feed horn wide half angle 55° beamwidth in the operating bandwidth of 30.5 – 50.5 GHz with minimum noise contribution. A wideband, low loss, HDPE window with two anti-reflection (AR) layers and excellent performance over the operating range is proposed in this paper.

1 Introduction

A dual linear polarization, single-feed Q-band cryogenic radio astronomy receiver with a compact front-end system and calibration noise injection module is under development at NRC Herzberg in Victoria, Canada. The proposed cryogenic receiver covers the frequency range of 30.5 – 50.5 GHz and has 16-Kelvin and 70-Kelvin stages.

The 16-K stage contains the feed horn, the OMT with two integrated 35 dB directional couplers for noise injection, and two low noise amplifiers (LNAs). The feed horn is positioned in the cold stage in order to reduce the noise, compared to an ambient-temperature feed, and removes the requirement to use a thermal transition between the feed and the cryogenic low noise amplifier [1]. The first optical component of the Q-band receiver is the vacuum window and a challenge that is addressed in this paper is the design of a high efficiency cryostat vacuum window that does not interfere with the wide 55° half-opening angle dictated by DVA-2 and ngVLA optic requirements [2].

This paper presents the design process, tolerance analysis, and specification of a vacuum window for the Q-band receiver.

2 Vacuum Window

The cryogenic Q-band receiver needs a vacuum window to transfer the radiated energy from sky to the 16-K cooled feed horn with minimum loss [3]. The goal is to keep the return loss of the window better than 25 dB and insertion loss better than 0.1 dB across the frequency range of 30.5 – 50.5 GHz. Figure 1 shows the electrical block diagram of the vacuum window.

Considering the dielectric constant, loss tangent, mechanical characteristics, and ease of fabrication high-density polyethylene (HDPE) is chosen as the vacuum window material for the Q-band receiver. The material properties of the HDPE that were used are $\varepsilon_r = 2.33$ and $\tan\delta = 2.5e - 04$ for EM simulation.

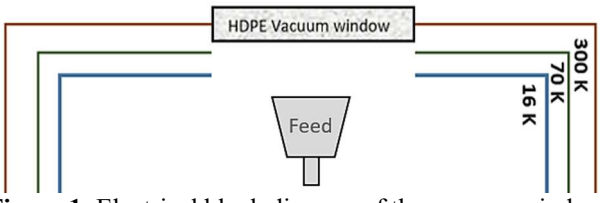

Figure 1. Electrical block diagram of the vacuum window.

The noise contribution of the vacuum window can be significant as the first component in receiver chain noise analysis. To calculate the noise added due to the vacuum window, the entire cascaded receiver noise analysis is presented in [3]. Based on the presented analysis and considering the attenuation of the signal by dielectric loss, the thickness of the HDPE window should remain 10 mm or thinner to keep the added noise smaller than 1 Kelvin.

3 Anti-reflection layer

A standard strategy to improve return loss is to add one or more anti-reflection layers. For an interface between two dielectric materials of refractive indexes n_1 and n_2, the ideal single anti-reflective layer has a refractive index of [4]:

$$n_m = \sqrt{n_1 * n_2} \qquad (1)$$

Multiple anti-reflection layers help to get a better match in a wider bandwidth. The frequency-domain (FD) solver of CST studio has been used for full-wave electromagnetic analysis. We modeled the window, including a flat HDPE layer and anti-reflection layers, using an infinite, periodic structure and then excited the ports with Floquet modes. The associated unit cell model with two ideal anti-reflection layers is shown in Figure 2 where a return loss of 25 dB has been achieved as the baseline.

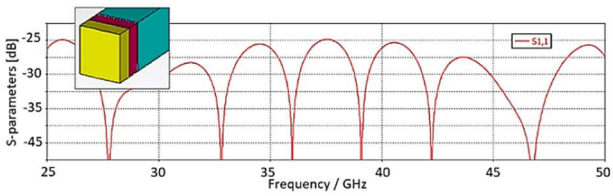

Figure 2. Reflection coefficient of two layers of ideal AR.

The anti-reflection layer can be created by machining into the surface of a dielectric sheet to create layers of different

effective dielectric constants. Machined features may take many shapes, including linear or concentric circular grooves, or arrays of different shapes like holes, stubs, or cones [5].

To find the suitable AR layer with minimum loss and best performance at Q-band frequency range, various structures including solid plate, cone, circular, and square hole shapes are investigated. Taking into account different shapes of AR layer, grid type (x-y grid vs hexagonal grid [3]), multiple AR layers (1, 2, and 3 layers), minimum loss, minimum effect on the radiation pattern of the feed horn, and ease of fabrication, a two-layer anti-reflection window with circular holes and the hexagonal grid was chosen for this project.

Based on theory explained in [6] to minimize diffraction from anti-reflection layer the pitch distance has to be:

$$p < \frac{\lambda}{(n_h + n_a \sin\theta_i)} \qquad (2)$$

Where n_h is the index of the substrate which here is HDPE index, n_a is the incident medium index which here is air index, θ_i is the angle of incident, P is the pitch value (centre to centre spacing between grooves), and λ is the wavelength. The proposed hexagonal layout is show in Figure 3 where the unit cell model is highlighted in the centre.

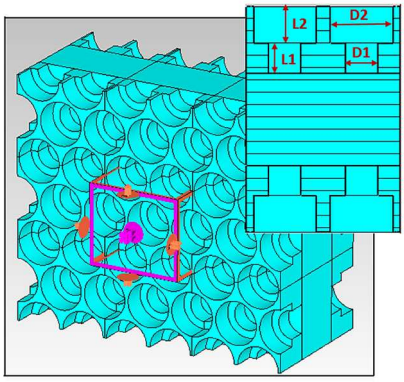

Figure 3. The proposed anti-reflection layer for the Q-band receiver. [D1=2mm, D2=3.1mm, L1=1.3mm, L2=1.6mm].

The log magnitude of reflection coefficient and insertion loss of the 10 mm thick window with two AR layers are shown in Figure 4 and Figure 5, respectively. As it is shown this design has a great performance with return loss better than 30 dB despite of the thickness of the window and insertion loss better than 0.02 dB from 30 to 51 GHz.

Since HDPE material parameters vary between manufacturers, a tolerance analysis using ±10% of nominal HDPE index of 2.33 and tan δ=2.5e-04 is done which is presented in Figure 6 and 7. As it is shown 10% variation in the HDPE material specification is a safe margin for the proposed design and does not have any significant effect on the designed AR layer.

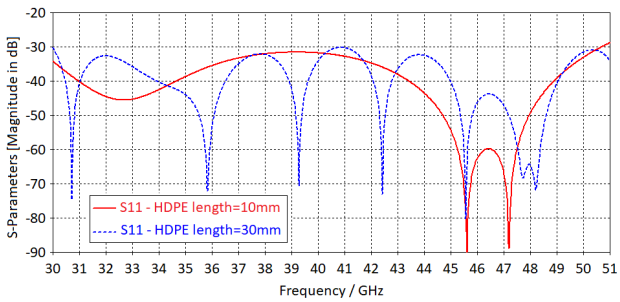

Figure 4. The return loss of the proposed AR layer for two different HDPE thickness, 10 mm vs. 30 mm.

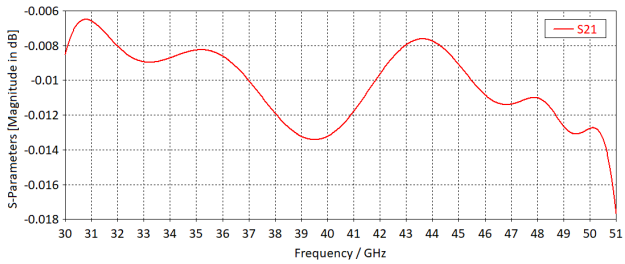

Figure 5. The insertion loss of the proposed AR layer with 10 mm thickness.

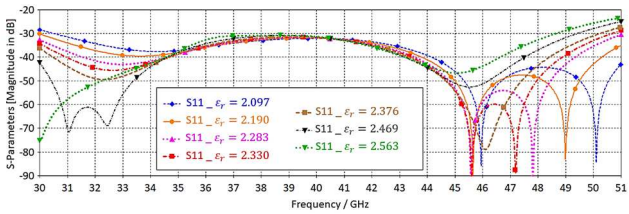

Figure 6. Tolerance analysis of HDPE permittivity ±10% of the nominal values.

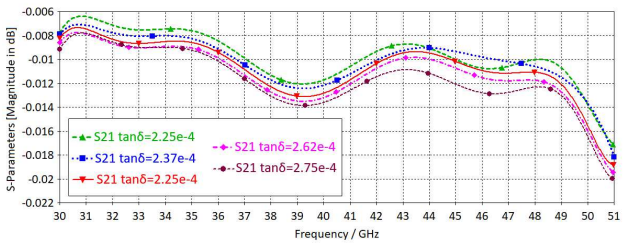

Figure 7. Tolerance analysis of HDPE loss ±10% of the nominal values.

4 Vacuum Window structure

The diameter of the window is a highly important parameter since it may limit overall aperture efficiency due to truncation. A smaller window would be advantageous since it not only reduces the thermal loading but also decreases the mechanical stress and deflection under vacuum.

Both the ngVLA and DVA-2 telescope are carbon composite offset Gregorian which have a shaped optic with a wide half-angle opening (55-degree) that are designed to map a 16 dB edge taper on the secondary [2], [7].

Considering the abovementioned optics, an EM analysis including aperture efficiency, electric field distribution, and far-field radiation pattern is done on a number of different diameters to find the optimum value. The vacuum window plus feed horn and the metal box around the structure acting as dewar walls are modeled and simulated in CST as is depicted in Figure 8.

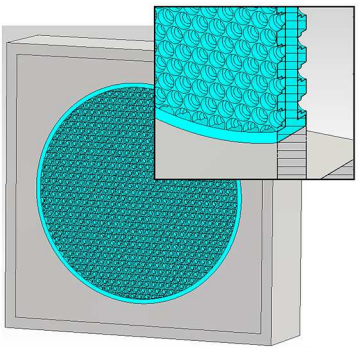

Figure 8. Vacuum window structure.

Figure 9 to Figure 11 present a parametric study of four different diameters while keeping the distance between the radiating element and window constant at 4 mm.

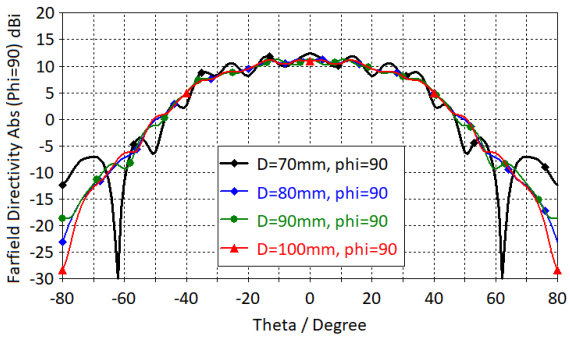

(a)

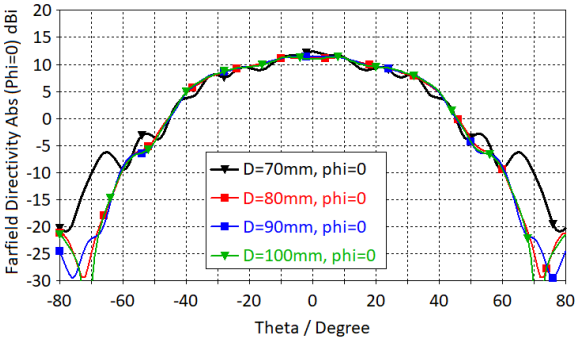

(b)

Figure 9. Farfield radiation pattern of the vacuum window at four different diameter values at (a) E-plane, (b) H-plane.

As it is shown in Figure 9, the window diameters smaller than 80 mm do not provide a smooth pattern on the main lobe and there is clear truncation resulting in severe beam ripple. As shown in Figure 10, the aperture efficiency degrades about 3% due to truncation using the smallest diameter of 70 mm. There is some fluctuation apparent within Figure 10, especially at the mid-band frequency, when comparing between the horn itself and combined with the window. We suspect poor mesh resolution within the EM model and this will be investigated in the future.

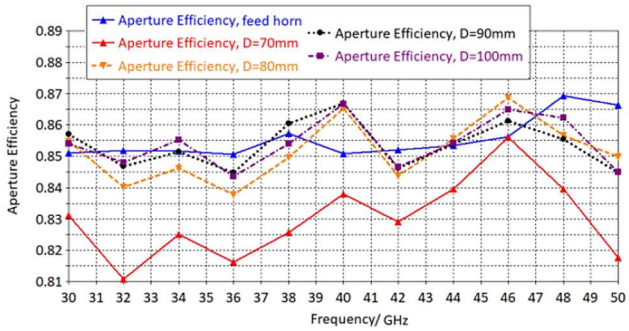

Figure 10. Aperture efficiency illustrating truncation effects for four different vacuum window diameters.

The electric field distribution of the feed horn through the vacuum window shown in Figure 11 illustrates the truncation resulting from a diameter smaller than 80 mm.

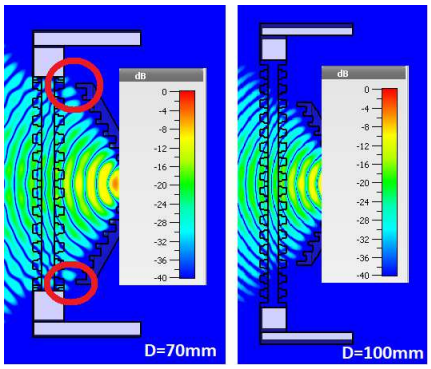

Figure 11. Electric field distribution through the vacuum window at D=70 mm (left) and D=100 mm (right).

Therefore, for the given feed horn position, the smallest suggested diameter is 80 mm. A larger vacuum window is preferable if there are no mechanical design or cartridge volume constraints.

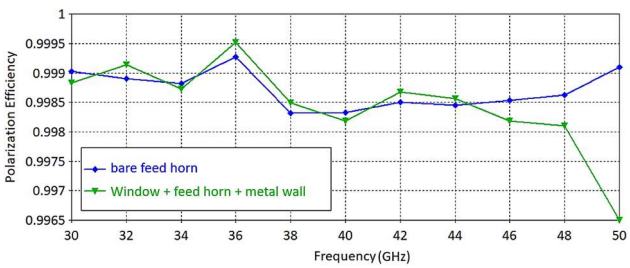

Figure 12. Polarization efficiency of a feed horn and vacuum window with 100 mm diameter + feed.

The refractive index of a material is dependent on the incident angle which may give rise to additional degradation in cross-polarization [5]. The cross-polarization of a bare feed horn (an optimized version of feed presented in [8]) and the structure shown in Figure 8 (which include feed + vacuum window + metal wall) are compared in Figures 12 and 13. The proposed AR layer does not have a significant effect on the cross-polarization

except in higher frequencies that polarization efficiency is 0.3% degraded which will be investigated in the future.

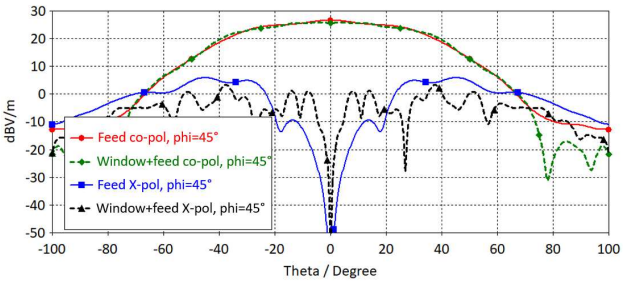

Figure 13. Comparison between bare horn and vacuum window + feed cross polarization levels at mid-band frequency 40 GHz with 100 mm diameter.

Using a window diameter of 100 mm and thickness of 10 mm, Figure 14 shows the reflection coefficient of the first five modes of the model. This model has a return loss better than 30 dB for 90% of the bandwidth and better than 20 dB in the entire operating frequency range. Higher order reflected modes have been simulated to be below -70 dB.

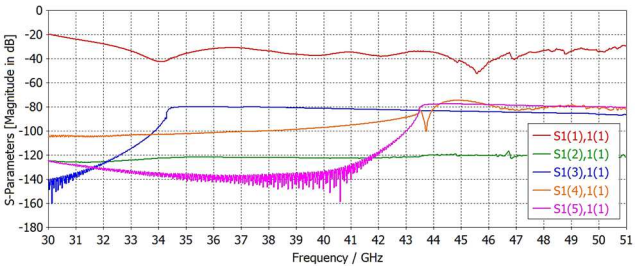

Figure 14. Reflection coefficient of the vacuum window (exciting first 5 modes).

The proposed vacuum window plus feed horn structure efficiency is calculated by applying a post-processing template within CST using a VBA macro. This calculation performs numerical integration over far-field radiation pattern to calculate its aperture efficiency following [9].

Figure 15 demonstrates the amplitude, polarization, phase, spillover, and combined aperture efficiency of the proposed vacuum window plus the flare horn used in Figure 12 and introduced in [8].

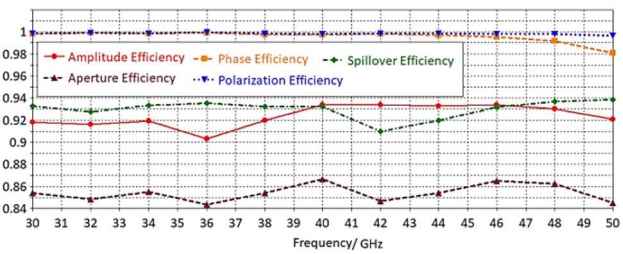

Figure 15. Efficiency calculations for a 100 mm vacuum window + feed horn.

5 Conclusion

A vacuum window covering the frequency range of 30 to 51 GHz is designed and presented in this paper. To obtain minimum loss and maximum efficiency the proposed design has two hexagonal circular hole anti-reflection layers on top and bottom of a flat HDPE layer with the total thickness of 10 mm.

Excellent performance with reflection loss better than 20 dB and aperture efficiency higher than 84% in the entire operating bandwidth are achieved. The proposed vacuum window will be built and measured for NRC Q-band receiver and a possible candidate for ngVLA-band-5 receiver.

6 References

[1] L. Locke, L. A. Baker, D. Henke, F. Jiang, L. B. G. Knee, V. Reshetov, "Q-band single pixel receiver development for the ngVLA and NRC," in Proc. SPIE 10708, Millimeter, Submillimeter, and Far-Infrared Detectors and Instrumentation for Astronomy IX, 1070832, July 2018.

[2] R. Selina et al., "System Reference Design," Nat. Radio Astron. Observatory, NRAO Doc. 020.25.00.00.00-0001-REQ-A-ANTENNA_PRELIM_TECH_REQS, ngVLA Reference Design, Vol. 1, Jul. 2019.

[3] S. Salem Hesari, D. Henke, V. Reshetov, F. Jiang, A. Seyfollahi, L. B. G. Knee, L. Baker, J. Bornemann, and D. Chalmers "Q-band receiver system design for the Canadian DVA-2 radio telescope", Proc. SPIE 11453, Millimeter, Submillimeter, and Far-Infrared Detectors and Instrumentation for Astronomy X, 114533A, December 2020.

[4] T. Morita and S. B. Cohn, "Microwave lens matching by simulated quarter-wave transformers," IRE Trans. Antennas Propag. 4, 33–39, 1956.

[5] V. Tapia, R. Rodriguez,N. Reyes, F.P. Mena, P. Yagoubov, F. Cuttaia, and L. Bronfman, "Systematic study of the cross polarization introduced by broadband antireflection layers at microwave frequencies," Applied Optics, Vol. 57, No. 31, Nov. 2018.

[6] R. Datta, C. D. Munson, M. D. Niemack, J. J. McMahon, J. Britton, E. J. Wollack, J. Beall, M. J. Devlin, J. Fowler, P. Gallardo, J. Hubmayr, K. Irwin, L. Newburgh, J. P. Nibarger, L. Page, M. A. Quijada, B. L. Schmitt, S. T. Staggs, R. Thornton, and L. Zhang, "Large-aperture wide-bandwidth antireflection-coated silicon lenses for millimeter wavelengths," Appl. Opt., 52 8747 (2013).

[7] L. Baker, W. A. Imbriale, "Optical Design of DVA-1, A Prototype Antenna for the SKA Mid-Band Array", 16th International Symposium on Antenna Technology and Applied Electromagnetics (ANTEM), 2014.

[8] D. Henke, S. Salem Hesari, L. Knee, "Axial Ring Feed Horn with Logarithmic Flare for Offset Gregorian Optics," submitted for publication in URSI GASS 2021, Rome, Aug. 28–Sept. 4, 2021.

[9] K. Pontoppidan, "Electromagnetic properties and optical analysis of the ALMA antennas and Front Ends," TICRA, S-1430-02, Oct. 2007.